# An improved method to measure the antenna resistance and radiated power of ICRF-antennas using current probes

H. Faugel[a], V. Bobkov[a], F. Braun[a], Th. Franke[a], D.A. Hartmann[b], M. Kircher[a], J.-M. Noterdaeme[a c], G. Siegl[a] and ASDEX Upgrade Team[a]

[a] *Max-Planck-Institut für Plasmaphysik, EURATOM Association, D-85748 Garching, Germany*
[b] *Max-Planck-Institut für Plasmaphysik, EURATOM Association, D-17491 Greifswald, Germany*
[c]*EESA Department, Ghent University, B-9000 Gent, Belgium*

The coupling properties of ICRF antennas depend on the plasma boundary characteristics, which are modified for example by H-Mode or ELMs. The impedance and the power into the antenna feeding line are measured with a pair of directional couplers near the double stub tuner matching system. Those measurements include the losses of the transmission line and the antenna. An approach to separate the radiated power from the losses is to measure the current in the antenna loops. To measure the current in the short of the antenna loop two current probes have been installed near the short of the antenna loops in one of the ICRF antennas during the 2009/2010 shutdown of ASDEX Upgrade. These signals allow a new approach in calculating the antenna resistance and the launched power and can be used to separate the launched power from the losses in the matching system and transmission lines up to the antenna. Although the calibration of the signal amplitude from the current probes needs further investigation, the amplitude is proportional to the current in the antenna loop. With those probes and a new real-time DSP-based system, the radiated (as opposed to the total power i.e. including loss power) power can be feedback controlled.

Keywords: ICRF, ASDEX Upgrade, Matching, Antenna, Transmission line

## 1. Introduction

The ICRF system at ASDEX Upgrade went into operation in 1992 and has contributed to making ICRF a reliable heating system on a divertor tokamak [1]. The implementation of a hybrid coupler system has been instrumental [2] on overcoming issues with reflected power caused by either L-H-Mode transitions or ELMs [3]. The reduction of reflected power to the generators and a workstation based shot-by-shot matching program in combination with a database in which the stub tuner positions for different plasma parameters are stored, made it possible to easily match to new plasma conditions. This matching program uses a simplified schematic describing transmission line and antenna for the matching procedure and has shown its reliability.

At the moment, the calculation of the total antenna resistance is done by measuring the power into matching system and antenna transmission line and using a selected voltage probe to measure the maximum voltage on the transmission line $U_{max}$. Evaluating the launched power of the antenna needs a characterization of the transmission line and antenna losses, which depend on the antenna resistance. During the 2009/10 shutdown of ASDEX Upgrade two current probes have been installed to enable a current measurement in the antenna.

## 2. Matching and transmission line losses

The matching system uses a double stub tuner system at each of the four antennas, each antenna is a double loop antenna [4]. In the recent years the antenna has been only modified in details like the cross section of the antenna loop to reduce edge electric fields, the addition of holes in the central conduction to allow better pumping, etc. In order to calculate the settings of the stub tuners for matching, directional couplers close to the double stub tuner system are used to measure forward and reflected power. For the calculation of matching a lossless model is sufficient, whereas the launched power calculation could be improved if transmission line losses were estimated more accurately.

To eliminate the transmission line losses from measurement a power measurement close to the antenna would be useful, but while directional couplers can give exact numbers of the forward and reflected power at relatively low VSWR (voltage standing wave ratio), at a high VSWR they fail because of their limited directivity. Here both directional couplers are showing about the same amplitude plus an error component caused by the directivity so that the calculation of forward and reflected power is prone to large errors. A calibration to get rid of these errors is possible but complicated [5].

Although the attenuation in the transmission lines of the ICRF-system is low, it can not be neglected. E.g. the 25 Ohm transmission line with 230 mm diameter of the outer conductor made out of aluminum and a 150 mm copper inner conductor, which is mainly used in the antenna feeding lines, shows an attenuation of about 0.001 dB/m at 30 MHz when matched. A mismatched transmission line has an increased attenuation, which can be calculated as following [6]:

*author's email: helmut.faugel@ipp.mpg.de*

$$p = 10 \log \frac{\left(1-\frac{R'}{Z}\right)-\left(\frac{s-1}{s+1}\right)^2}{\left(1-\frac{R'}{Z}\right)\left(1-\left(\frac{s-1}{s+2}\right)^2\right)}$$

where s is the standing wave ratio VSWR, R' is the resistance load and Z is the line impedance. As the antenna transmission line is not homogenous, the calculation of the real attenuation of the antenna feeding line has to take into account the different conductor materials and the different diameters used in the different sections. The conductivity of materials varies from $1.37 \times 10^6$ S/m for stainless steel 1.4541 up to $57 \times 10^6$ S/m for copper 2.0070. There are five different transmission line section incorporated in the whole antenna feeding line, which have different attenuations (see Table 1).

| Outer conductor | | Inner conductor | | |
|---|---|---|---|---|
| D (mm) | Material | d (mm) | Material | Att. (dB/m) |
| 230 | Al | 150 | Cu 2.0070 | $0.98 \times 10^{-3}$ |
| 230 | G-Al 5 Si Mg | 150 | G-Al 5 Si Mg | $1.52 \times 10^{-3}$ |
| 152 | Cu 2.0070 | 100 | Cu 2.0070 | $1.32 \times 10^{-3}$ |
| 152 | Cu 2.0070 | 100 | 1.4541 + 2 µm Au | $2.77 \times 10^{-3}$ |
| 152 | Cu 2.0070 | 100 | 1.4541 | $5.64 \times 10^{-3}$ |

Tab.1 Attenuation per meter for different types of matched 25 Ohm transmission line sections at 30 MHz.

The RMS surface roughness of 5 µm on the aluminum cast parts like the 90° elbows can be neglected in the ICRF frequency range. The total attenuation including dielectric losses in the ceramics at 30 MHz and a VSWR of 6 varies than between 0.076 dB (1.73 % loss) and 0.086 dB (1.97 % loss) for the antenna feeding line for a arbitrary phase variation. The loss for a matched line is 0.026 dB (0.60 %).

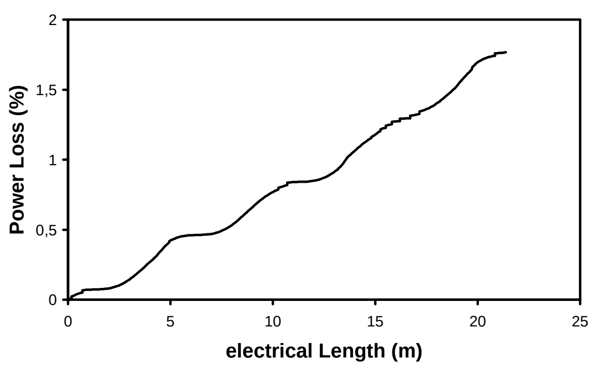


Fig. 1 Accumulated power loss along an antenna transmission line for a VSWR of 6 form the matching system till the antenna connection

Fig.1 shows the losses of a typical antenna transmission line used at ASDEX Upgrade along its electrical length for a VSWR of 6, which is quite common. To perform the calculation, the transmission line was divided from the output of the matching system till the end of the vacuum feedthrough line into short sections with a maximum length of 0.1 m. The different characteristics of the lines like conductivity and diameters of inner and outer conductor were used to calculate the ohmic losses according to the actual current in that line section. This ohmic loss was then subtracted from the input power in this section, and this power level served as the input to the next section, where the actual power was used to calculate the properties of the next section. The dielectric losses were calculated using the voltage at the position of the ceramic, whereby the equivalent length of the ceramics was calculated based on results of a simulation with HFSS [7]. The values for permittivity and dielectric loss tangent were taken from the manufacturer data sheets. The power lost in the ceramic was subtracted in the same way as was done for the ohmic losses. The waviness of the accumulated losses is due to the current distribution along the line which causes higher losses at the current maxima, whereas the small steps in the flat parts of the curve are caused by dielectric losses of the supporting ceramics because of the high voltage at this position. All this considerations have been made without taking care of harmonics on the transmission line, which are present. E.g. the average power dissipation in the ceramics can be up to 25 % higher when a second harmonic (3f) with a level of 20 dB below the fundamental is present, which is about the expected level of harmonic content.

## 3. Antenna loss calculation

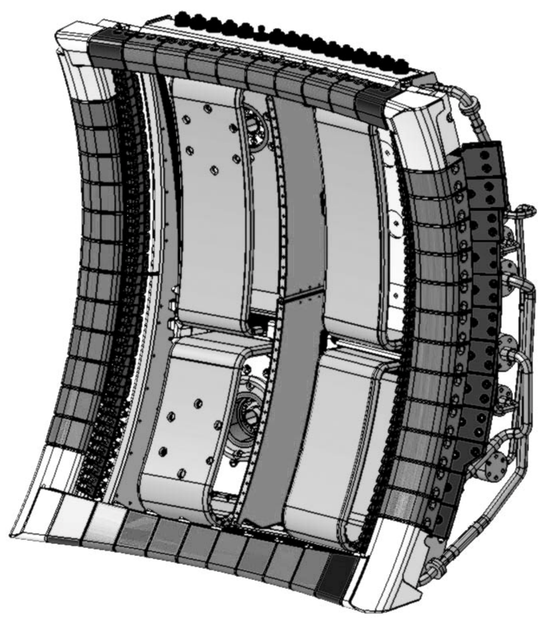

Fig. 2 View of a ASDEX Upgrade ICRF antenna with limiters and removed Faraday screen.

The total loss resistance of the antenna (see Fig. 2) plus transmission line has been determined from the measurements of the $U_{max}$ probes and the power into the matching system in vacuum conditions. The values for antenna 4, which is the antenna equipped with the current probes, are 340 mOhm for the left (seen from the plasma side, Fig. 3) and 480 mOhm for the right antenna loop at 30 MHz. These values include the calculated transmission line resistivity of 140 mOhm and the calculated dielectric losses which can be converted to a resistance of about 80 mOhm. Taking that into account, the loss resistance for the antenna is 120 mOhm for left loop and 260 mOhm for the right one. The higher resistance for the right loop is probably caused by the additional strip line needed to feed the loop. This difference will cause some unbalance in the current distribution at low radiation resistance. A simplified schematic of the total resistive load at the end of the antenna transmission line consists of two resistors in series: $R_{rad}$ for the radiation resistance and $R_{loss}$ for the antenna losses. The losses for the radiation resistance of 4 Ohm per antenna loop are 2.9 % for the left loop and 6.1 % for the right loop. As the power into each of the antenna loops is about half of the total power, the overall loss is averaged to 4.5 % for the whole antenna. The total loss of the transmission line and the antenna at these conditions is 6.6 % of the power input. What remains unknown at the moment is how much power is lost in the Faraday screen, the limiters and other structures near the antenna.

## 4. Shunt measurement

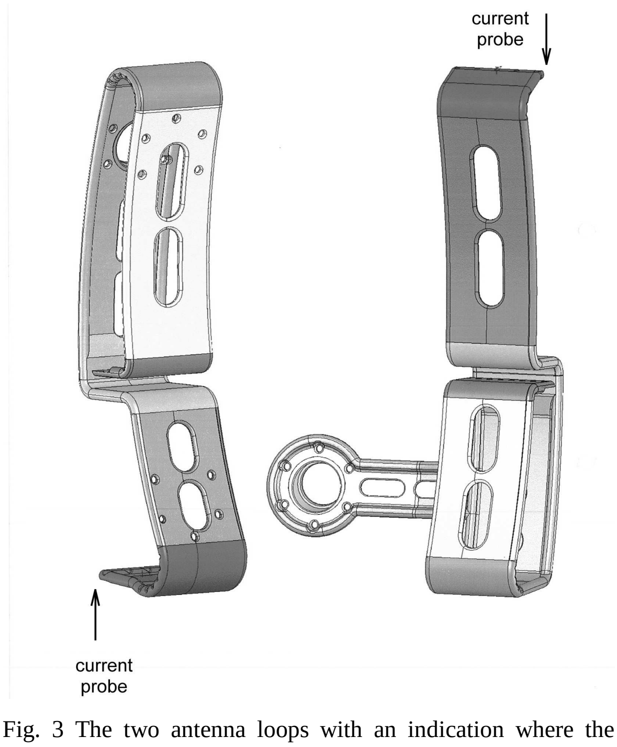


Fig. 3 The two antenna loops with an indication where the current measurement was installed.

During the opening of ASDEX Upgrade 2009/10 two small UT-085 semi-rigid coax cables have been installed near one of the short circuits of each antenna strap. The outer conductor of the coax cable was mounted and connected to the antenna backplate on top of a small block, itself connected to the back plate, while the inner conductor was connected to the antenna strap with a small hole, forming a mechanically short (approximately 18 mm long for the left loop and approx. 20.5 mm long for the right antenna loop) shunt resistor (Fig. 4). A comparison of the measured rf-voltage with the calculated resistance showed that even this short piece of the antenna loop can not be treated as a simple resistor. The resistance of this antenna part calculated as a two thin conducting parallel sheets with a width of 180 mm gave at 30 MHz a value of 465 µOhm for the left and respectively 530 µOhm for the right antenna loop. As the measured voltage at this position is in the range of some Volts, these resistances would be equal to currents in the kA range, which does not match the calculations of the expected currents derived by $U_{max}$ and input power. A calculation of the induced voltage by treating the small gap between antenna short and connection of the semi-rigid cable as a coupling loop with an area of 20 $mm^2$ gave a voltage of 0.47 V at 30 MHz and a current of 100 A, which does also not explain the measured voltages. The reason for this large difference is not known, but could be related to the remaining self-inductance of the contact piece. A HFSS simulation of these parts is necessary to understand and calculate this.

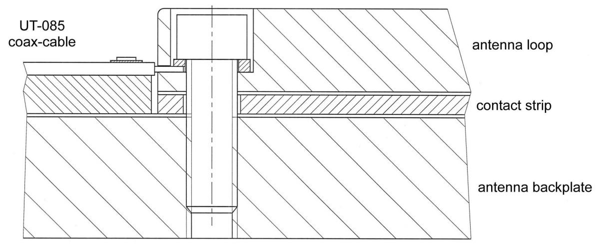


Fig. 4 Cross section of the probe setup.

Fig. 5 shows the comparison of the shunt signals with a signal calculated from the voltage maximum probe and the forward-minus-reflected power into the antenna 4 setup. The correlation is very good, which indicates that the shunt signal can be used as signal which is proportional to the maximum current in the antenna. The calculation of the line impedance $Z_L$ by dividing $U_{max}$ by $I_{max}$ also gave a very good correlation. A phase measurement between the two current probes showed no dependence on the antenna resistance or applied rf-power. The reason for the quite high noise level on the resistance calculated from current signal is that the rf-detector for the current signal was not equipped with a 10 MHz high-pass filter.

The measurement of $U_{max}$ has some uncertainties, as for each of frequency a different voltage probe has to be selected to be at (near) the maximum. The probes are placed 0.25 m apart, and even at fixed frequency a phase shift of the antenna impedance can change the position of voltage maximum significantly. The advantage of deriving the antenna resistance and antenna losses from a current signal measured at the short of the antenna is that one does not need any transmission line transformations with uncertain or frequency dependent electrical lengths and a possible phase shift which depends on the antenna coupling. What can be also seen in Fig. 5 is that the power which can be applied to the antenna is largely

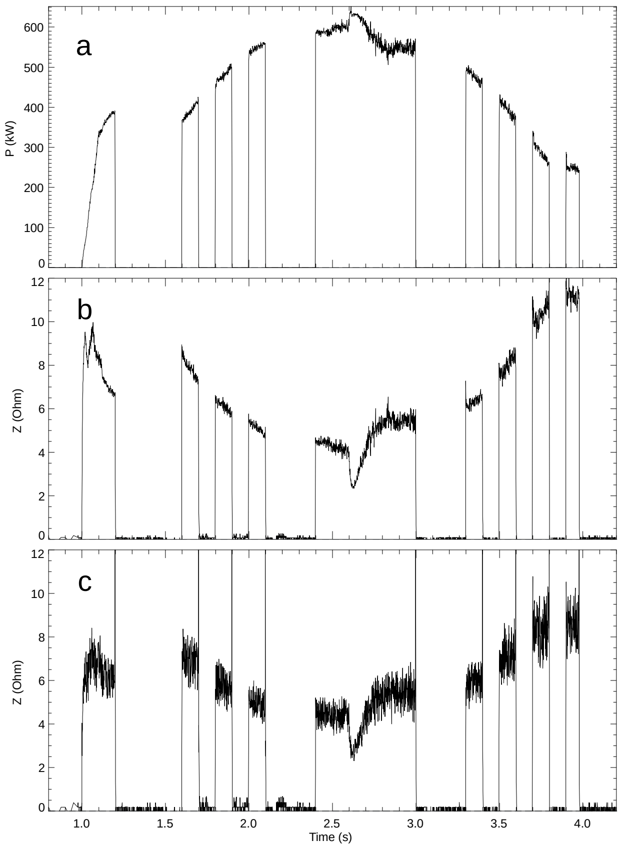


Fig.5 Shot #25635: The traces show (a) the input power to antenna 4 matching system and the (b) antenna impedance of the left antenna loop calculated using the $U_{max}$ probe and the antenna current probe (c). The peaks in lowest trace are artifacts caused by different sampling speeds.

limited by the change of antenna impedance during a shot. During this shot the plasma – antenna distance was varied which led to large changes in the coupling. As the stub tuner of the matching system can only match to one impedance a large portion of the power is reflected at the input of the matching system. To be able to maintain a constant radiated power (cancel the loss of ICRF power due to changing antenna resistance) a feedback system is being put into operation.

## 5. DSP-based signal generator

A new signal generator is now replacing the old CAMAC based system. It will give us much more flexibility on the control of the ICRF-power and the anode voltage of the generator final stage. The system is based on a Keithley ADwin system, with 16 analog inputs and 8 analog outputs, 8 digital inputs and 8 digital outputs and up to 4 trigger inputs. It can store up to 32k samples per channel, which can be used as an arbitrary waveform generator with an output speed of 2k samples/s. This is sufficient since the amplitude modulation input of the rf-generator has a bandwidth of about 500 Hz. The signal generator is connected via Ethernet to the data acquisition workstation and can be programmed in ADbasic allowing real-time feedback control. At the moment, the system is used to provide a stored waveform which controls the output power and anode voltage of the rf-generators, but in the near future it should fulfill feedback tasks. A number of feedback tasks are possible which can either help finding a good matching by limiting the reflected power at the generator output to levels which does not trigger safety system of the generator or preventing arcs in the antenna transmission by limiting the maximum voltage on the antenna transmission line with an active control of the generator power. A feedback of the anode voltage according to the anode dissipation and the screen grid current could help to sustain maximum output power of the generators [8]. As Fig. 5 shows, the input power into the matching system does vary as the plasma coupling changes. For this case, a feedback control which keeps the coupled power constant would be of great use for experiments which relay on constant conditions.

## Conclusions

The installation of current probes in the antenna short circuits seem to give a good measurement of $I_{max}$ which is probably a more reliable base for antenna resistance calculation than the currently used $U_{max}$ voltage probe. Calculations have shown that the loss in the transmission line is of the order of a few percent under typical conditions and that the loss inside of the antenna is about three times higher than that. For long pulse, ICRF systems cooling of transmission line components and the antenna will be a necessity.

## Acknowledgments

We want to thank J. Kneidl for exploring the depths of the ASDEX Upgrade experiment hall to confirm the transmission line components used in the antenna feeding line are in agreement with the drawings.

## References


[1] Noterdaeme J.-M., Hartmann D., et al. Comparing high power ion cyclotron resonance frequency heating with neutral injection in ASDEX Upgrade: differences, similarities and synergies. In: 17th IAEA Conf. on Fusion Energy, Yokohama, Japan IAEA,1998

[2] Noterdaeme J.-M., Wukitch S., Hartmann D.A., Brambilla M. et al. ICRF heating results in ASDEX Upgrade and W7-AS. In: The 16th IAEA Conf. on Fusion Energy, Montreal, IAEA, 1996

[3] V. Bobkov, Influence of ELMs on operation of ICRF antennas in ASDEX Upgrade, Journal of Nuclear Materials, 337 – 339 (2005) 776 – 780.

[4] Noterdaeme J.-M, Wesner F., Brambilla M., Fritsch R. Kutsch H.-J., Söll M., the ICRH team. The ASDEX Upgrade ICRH antenna, Fusion Engineering and Design 24 (1994) 65-74

[5] A. Fantom, Radio Frequency & Microwave Power Measurement, Peter Peregrinus Ldt, London, 1990, pp. 178ff.

[6] The American Radio Relay League, The ARRL handbook for radio amateurs 1996, pp 19.4–19.6

[7] F. Braun, D.A. Hartmann, Internal memos on results of the simulation of transmission lines with ceramics

[8] Imboden Ch., Schminke W., Wyss J. 2 x 2 MW ICRH Amplifier System, Proceedings of the 18th SOFT, Karlsruhe, 1994, p. 553-556